


# Longitudinal transcriptomic analysis of mouse sciatic nerve reveals pathways associated with age-related muscle pathology

Nicole Comfort<sup>1\*</sup> , Meethila Gade<sup>1</sup>, Madeleine Strait<sup>1</sup>, Samantha J. Merwin<sup>1</sup>, Daphne Antoniou<sup>2</sup>, Chiara Parodi<sup>1</sup>, Lina Marcinczyk<sup>1</sup>, Lea Jean-Francois<sup>1</sup>, Tessa R. Bloomquist<sup>1</sup>, Anna Memou<sup>3</sup>, Hardy J. Rideout<sup>3</sup>, Stefania Corti<sup>4</sup>, Shingo Kariya<sup>5</sup> & Diane B. Re<sup>1,6,7\*</sup>

<sup>1</sup>Department of Environmental Health Sciences, Mailman School of Public Health, Columbia University, New York, NY, USA; <sup>2</sup>Center for Basic Research, Biomedical Research Foundation of the Academy of Athens, Athens, Greece; <sup>3</sup>Center for Clinical, Experimental Surgery, and Translational Research, Biomedical Research Foundation of the Academy of Athens, Athens, Greece; <sup>4</sup>Neuroscience Section, Dino Ferrari Centre, Department of Pathophysiology and Transplantation, University of Milan, Milan, Italy; <sup>5</sup>Department of Neurology, Vagelos College of Physicians and Surgeons, Columbia University, New York, NY, USA; <sup>6</sup>Center for Motor Neuron Biology and Disease, Columbia University, New York, NY, USA; <sup>7</sup>NIEHS Center for Environmental Health Sciences in Northern Manhattan, Columbia University, New York, NY, USA

## Abstract

**Background** Sarcopenia, the age-associated decline in skeletal muscle mass and strength, has long been considered a disease of muscle only, but accumulating evidence suggests that sarcopenia could originate from the neural components controlling muscles. To identify early molecular changes in nerves that may drive sarcopenia initiation, we performed a longitudinal transcriptomic analysis of the sciatic nerve, which governs lower limb muscles, in aging mice.

**Methods** Sciatic nerve and gastrocnemius muscle were obtained from female C57BL/6JN mice aged 5, 18, 21 and 24 months old ( $n = 6$  per age group). Sciatic nerve RNA was extracted and underwent RNA sequencing (RNA-seq). Differentially expressed genes (DEGs) were validated using quantitative reverse transcription PCR (qRT-PCR). Functional enrichment analysis of clusters of genes associated with patterns of gene expression across age groups (adjusted  $P$ -value  $< 0.05$ , likelihood ratio test [LRT]) was performed. Pathological skeletal muscle aging was confirmed between 21 and 24 months by a combination of molecular and pathological biomarkers. Myofiber denervation was confirmed with qRT-PCR of *Chrnd*, *Chrng*, *Myog*, *Runx1* and *Gadd45a* in gastrocnemius muscle. Changes in muscle mass, cross-sectional myofiber size and percentage of fibres with centralized nuclei were analysed in a separate cohort of mice from the same colony ( $n = 4$ – $6$  per age group).

**Results** We detected 51 significant DEGs in sciatic nerve of 18-month-old mice compared with 5-month-old mice (absolute value of fold change  $> 2$ ; false discovery rate [FDR]  $< 0.05$ ). Up-regulated DEGs included *Dbp* ( $\log_2$  fold change [LFC] = 2.63, FDR  $< 0.001$ ) and *Lmod2* (LFC = 7.52, FDR = 0.001). Down-regulated DEGs included *Cdh6* (LFC =  $-21.38$ , FDR  $< 0.001$ ) and *Gbp1* (LFC =  $-21.78$ , FDR  $< 0.001$ ). We validated RNA-seq findings with qRT-PCR of various up- and down-regulated genes including *Dbp* and *Cdh6*. Up-regulated genes (FDR  $< 0.1$ ) were associated with the AMP-activated protein kinase signalling pathway (FDR = 0.02) and circadian rhythm (FDR = 0.02), whereas down-regulated DEGs were associated with biosynthesis and metabolic pathways (FDR  $< 0.05$ ). We identified seven significant clusters of genes (FDR  $< 0.05$ , LRT) with similar expression patterns across groups. Functional enrichment analysis of these clusters revealed biological processes that may be implicated in age-related changes in skeletal muscles and/or sarcopenia initiation including extracellular matrix organization and an immune response (FDR  $< 0.05$ ).

**Conclusions** Gene expression changes in mouse peripheral nerve were detected prior to disturbances in myofiber innervation and sarcopenia onset. These early molecular changes we report shed a new light on biological processes that may be implicated in sarcopenia initiation and pathogenesis. Future studies are warranted to confirm the disease modifying and/or biomarker potential of the key changes we report here.

**Keywords** aging; frailty; motor unit; RNA-seq; sarcopenia; skeletal muscle

Received: 25 March 2022; Revised: 5 February 2023; Accepted: 8 February 2023

\*Correspondence to: Nicole Comfort, Department of Environmental Health Sciences, Mailman School of Public Health, Columbia University, New York, NY, USA.

Email: [nicole.comfort@columbia.edu](mailto:nicole.comfort@columbia.edu);

Diane B. Re, NIEHS Center for Environmental Health Sciences in Northern Manhattan, Columbia University, New York, NY, USA. Email: [dr2240@cumc.columbia.edu](mailto:dr2240@cumc.columbia.edu)

## Introduction

Based on its symptomatic and histological features, sarcopenia, the age-associated loss in skeletal muscle mass and strength, has long been considered a disease of skeletal muscle fibres only. However, accumulating evidence suggests that sarcopenia could originate from the neural components controlling muscle strength and hence be defined as a neuromuscular disease.<sup>1–3, S1</sup> Although current evidence suggests that motor nerves and presynapses of neuromuscular junctions (NMJs) could be implicated in sarcopenia pathophysiology, their role in sarcopenia initiation has not been fully elucidated.

We hypothesized that sarcopenia initiation and its early molecular programming could be captured in the major nerve of the lower limb, the sciatic nerve, reflected by changes in gene expression in nerves preceding myofiber denervation or sarcopenia development in muscle. Most previous gene expression profiling studies investigating the mechanisms of sarcopenia pathophysiology have been limited by their use of microarrays for peripheral nerve molecular profiling. Microarrays cover only a defined set of transcripts, have high background levels due to cross-hybridization and have a limited dynamic range due to both background and saturation of signals. However, studies that utilized next-generation sequencing technologies have so far focused on age-related changes in muscles rather than nerves.<sup>4</sup>

To circumvent these issues and capture early molecular events responsible for the initiation of sarcopenia, we performed deep RNA sequencing (RNA-seq)<sup>S2</sup> of sciatic nerves, isolated at different time points from healthy mature adult (5 months), late middle-aged (18 months), 'old' (21 months) and 'very old' (24 months) mice.<sup>S3</sup> Our objective was to identify early changes in gene expression related to the development of sarcopenia via transcriptomic profiling of aging sciatic nerves *in vivo*. In agreement with a potential neurogenic origin of sarcopenia, we identified a series of relevant gene expression changes in mouse peripheral nerve prior to signs of myofiber denervation and overt clinical onset of sarcopenia in muscles. Among the early molecular events that we report at 18 months, we confirm the importance of biological processes previously linked to sarcopenia while also reporting new findings that shed light on other pathophysiological mechanisms that may be implicated in sarcopenia initiation and pathogenesis. To our knowledge, this study is the first to utilize untargeted RNA-seq to investigate the

transcriptome of sciatic nerves in the context of sarcopenia. Future studies are warranted to validate which genes identified in the nerves are phenotypic drivers with potential implications for sarcopenia prevention and therapy.

## Methods

### *Mice and sample collection*

Female C57BL/6JN mice, derived from a strain that has previously been extensively characterized for the development of sarcopenia,<sup>5,6</sup> were obtained from the National Institute on Aging (NIA) mouse colony 2 weeks before turning 5, 18, 21 and 24 months old. The mice were kept in the Columbia University Medical Center animal facility for 2 weeks and then were used immediately. Mice had free access to the standard pellet and water diet and were maintained under a constant 12-h light/dark cycle at an environmental temperature of 21–23°C. All animal procedures complied with the Guide for the Care and Use of Laboratory Animals and were approved by the Columbia University Institutional Animal Care and Use Committee (Approval ID: AC-AAAN8900).

At 5 (mature adult negative control), 18 (late middle-aged), 21 (old) and 24 (very old) months, mice ( $n = 6$  per age group) were euthanized via deep anaesthesia followed by decapitation. We dissected both the right and left sciatic nerves following the method described by Bala and colleagues<sup>S4</sup> to ensure harvesting the maximum length of sciatic nerve from a point close to its origin in the sacral area through the popliteal fossa of adult mice. Freshly dissected sciatic nerves immediately underwent RNA extraction. For one of the legs, the lower portion was cut at the knee joint and was snap-frozen in liquid nitrogen and stored at  $-80^{\circ}\text{C}$  for later RNA extraction. For muscle morphological analyses, fresh frozen gastrocnemius (innervated by the sciatic nerve) and quadriceps (selected to assess a muscle with innervation by a different nerve, *i.e.*, the femoral nerve) muscles were obtained from a separate cohort of C57BL/6JN female mice (same age groups: 5, 18, 21 and 24 months) from the same NIA mouse colony ( $n = 6$  per age group). Mice were weighed immediately after euthanasia and freshly dissected gastrocnemius and quadriceps muscles were weighed individually before being flash frozen and stored at  $-80^{\circ}\text{C}$ . Other flash frozen organs collected from the same mice (*e.g.*, brain, liver

and kidney) are now available at the NIA rodent tissue bank to other investigators.

## Histology

Frozen gastrocnemius and quadriceps muscles were cut at the muscle mid-belly in two pieces before embedding in moulds (Fisherbrand™ Disposable Base Molds, Thermo Fisher Scientific) with Thermo Fisher Scientific Scigen Tissue-Plus™ O.C.T. Compound (Cat # 23-730-571). Cryosections (10 µm thick) of the mid-belly region of muscles were prepared. Then, frozen sections of gastrocnemius and quadriceps muscles were stained with an automated stainer set-up following the haematoxylin and eosin (H&E) staining method policy and standard operating procedures of the Histology Laboratory in the Department of Pathology at Columbia University Medical Center.

## Image acquisition and analysis

H&E-stained muscles were imaged using a Leica DMI8 microscope (with a 3.1-MP Leica EC3 camera). Pictures of the muscles were taken using the Leica LAS EZ imaging software. For each animal ( $n = 4$  per age group), seven pictures were taken at  $\times 20$  magnification. Gastrocnemius and quadriceps muscle mid-belly cross-section fibres were manually measured using the freehand section tool in ImageJ software to encircle individual myofibers. The minimal 'Ferret's diameter' (i.e., the minimum distance of parallel tangents at opposing borders of the muscle fibre, measured in microns)<sup>S5</sup> was calculated for each whole myofiber present in a picture. Approximately 300–600 myofibers were measured per animal. The number of myofibers with centralized nuclei was counted and expressed as a percentage of the total myofiber number. Image and morphometric examinations were performed by three independent, blinded investigators.

## Analysis of muscle weights and histology

A one-way analysis of variance (ANOVA) was used to test for any potential differences in the muscle weights (in grams, normalized to body weight or non-normalized) across age groups followed by Tukey's test. We report significant differences ( $P < 0.05$ ) for any pairwise comparison. For the histological analyses, potential differences across age groups in the number of centralized nuclei (expressed as a percentage of the total myofiber number) were assessed using the Kruskal–Wallis test followed by Dunnett's post hoc test (with 5 months serving as the reference group). In addition, we evaluated whether the distributions of the minimal 'Ferret's diameter' (measured in microns) differed across age groups<sup>S5</sup>

by performing the Kolmogorov–Smirnov test. Separate tests were performed for the gastrocnemius and quadriceps muscles. All analyses were two-sided with  $\alpha = 0.05$  and were performed in R (Version 4.1.1).

## RNA extraction

### Sciatic nerve

Total RNA was isolated from freshly dissected sciatic nerves using the Invitrogen PureLink™ RNA Mini Kit (Cat # 12183018A) following the manufacturer's protocol for  $\leq 10$  mg of fresh soft animal tissue (without the optional DNase treatment). All samples had total RNA concentration and RNA integrity numbers (RINs) assessed prior to sequencing or quantitative reverse transcription PCR (qRT-PCR). RINs were evaluated using an Agilent 2100 Bioanalyzer. After excluding two samples with low RIN (6.2) and low mapping, RINs ranged from 7.2 to 9.6 (Table S1). Exclusion of these two samples resulted in a total of 22 samples included in the final analysis.

### Gastrocnemius muscle

The gastrocnemius muscles were dissected from the leg on dry ice and 50 mg of tissue was flash frozen in duplicate. The tissue samples were then placed in a pre-chilled Eppendorf tube and homogenized with a Qiagen TissueRuptor II (Cat # 9002755) with disposable probes (Qiagen, Cat # 990890). Total RNA extraction was performed using TRIzol–chloroform extraction followed by column centrifugation using the Invitrogen PureLink™ RNA Mini Kit following the manufacturer's instructions. Then, samples were treated with DNase followed by wash buffer and eluted in water. Total RNA was quantified using the RiboGreen™ RNA Quantitation Kit (Thermo Fisher, Cat # R11490).

## Library preparation and RNA sequencing

Libraries were constructed at the Columbia Biomedical Core Facility. Briefly, mRNA was enriched from total RNA via poly-A pull-down using the Illumina TruSeq Stranded mRNA kit according to the manufacturer's instructions. Libraries were  $2 \times 100$  base-pair (bp) paired-end sequenced for each sample on an Illumina HiSeq4000 using 75-cycle High Output Kits (target 60 million reads per sample; see Data S1) at the Columbia University Genome Center. The data discussed in this publication have been deposited in NCBI's Gene Expression Omnibus<sup>S6</sup> and are accessible through GEO Series Accession Number GSE198669 (<https://www.ncbi.nlm.nih.gov/geo/query/acc.cgi?acc=GSE198669>).

## RNA sequencing analysis, quality control and identification of differentially expressed genes

We used RTA (Illumina) for base calling and bcl2fastq2 (Version 2.17) for converting BCL to fastq format, coupled with adaptor trimming. Quality control of the raw and trimmed reads was performed using FastQC and MultiQC.<sup>57, 58</sup> We aligned trimmed reads that passed quality control (Phred score > 30) to the mouse reference genome and transcriptome annotation (mm10, UCSC) using STAR aligner (Version 2.5.2b)<sup>59</sup> and quantified the reads that aligned uniquely to the transcriptome using featureCounts (v1.5.0-p3).<sup>510</sup> Sequencing yielded libraries with an average size of 39 million reads after alignment (*Data S1*). We removed one sample with an RIN < 7.0 from downstream analysis and a sample with low percentage of mapped reads (37%), resulting in a total of  $N = 22$  samples included in final analyses.

We used the DESeq2 (Version 1.34.0) package for R (Version 4.1.1; R-project.org/)<sup>511</sup> for further quality control, exploratory data analysis and differential expression analysis. For sample-level quality control, we conducted principal component analysis (PCA) of the RNA-seq data by first normalizing the counts for each sample using size factors obtained from DESeq2, log-transforming the normalized counts (using the regularized-logarithm [rlog] transformation) and computing the principal components of the resulting matrix using the plotPCA function of DESeq2 (*Figure S1*).

We removed 4716 (20.1%) rows of the DESeqDataSet that had no counts or only a single count across all included samples ( $N = 22$ ). We additionally specified that at least 4 samples have a count of 10 or higher, resulting in removal of an additional 2770 genes (11.8%). In total, 7486 (31.97%) of 23 416 unique genes were filtered out, resulting in 15 930 genes analysed in the DESeqDataSet. DESeq2 fits negative binomial generalized linear models for each gene and determines differential expression for pairwise comparisons by applying the Wald test for significance testing. Adjusted  $P$ -values were calculated by the Benjamini–Hochberg false discovery rate (FDR). We considered genes that had an absolute value of a  $\log_2$  fold change (LFC) > 1.0 with FDR  $q$ -value < 0.05 to be differentially expressed genes (DEGs).

## Validation of differentially expressed genes with quantitative reverse transcription PCR

### SYBR® Green reverse transcription PCR

For select genes in sciatic nerve identified as differentially expressed by DESeq2, we validated the RNA-seq results using qRT-PCR. We also performed qRT-PCR of the genes *Chrnd*, *Chrng*, *Gadd45a*, *Myog* and *Runx1* in gastrocnemius muscle to confirm NMJ denervation. Qiagen QuantiTect Primers (*Table S2*) were reconstituted in Tris-EDTA (TE) buffer (pH 8.0). The reverse transcription reaction was performed

using the Promega GoScript™ Reverse Transcriptase kit (Cat # PRA5000) for a reaction volume of 20  $\mu$ L. This was followed by SYBR® Green RT-qPCR reaction using KiCqStart™ SYBR® Green qPCR ReadyMix™ (Millipore Sigma, Cat # KCQS00). Briefly, 5  $\mu$ L of reaction mix was prepared using 2.5  $\mu$ L of qPCR ready mix, 1.25  $\mu$ L of sample cDNA and 1.25  $\mu$ L of primers. The RT-PCR reaction was run on Bio-Rad CFX384 Touch Real-Time PCR System as per kit instructions for three technical replicates.

### Quantitative reverse transcription PCR data analysis

RT-PCR results were analysed in RStudio (Version 3.6.0). Data were cleaned by excluding samples with cycle threshold (Ct) values > 35 and only 1 read per technical replicate. Raw Ct values were then normalized to the geometric mean of housekeeping genes (*Ppia* and *Hprt*, *Figure S2*; raw Ct values for each gene are shown in *Figure S3*). The resulting delta Ct (dCt) values were further normalized to the 5-month age group, which served as the reference, to create delta–delta Ct (ddCt) values. Only the raw dCt values were plotted for assays with many non-detects in the reference group (e.g., *Myog* in nerve). For the muscle assays, a one-way ANOVA was used to test for any statistically significant differences between the groups followed by post hoc analysis using the Dunnett test. We report significant differences in ddCt comparing each group (18, 21 and 24 months) to the reference group (5 months). For the nerve assays, we performed a one-way ANOVA followed by Tukey's test and report significant differences ( $P < 0.05$ ) for any pairwise comparison.

## Pattern identification

We analysed all pairwise comparisons simultaneously using the likelihood ratio test (LRT) in DESeq2 to identify any genes that showed an interesting change in expression across the different groups (5, 18, 21 and 24 months). We subset the rlog-transformed normalized counts to contain only genes significant with adjusted  $P$ -value < 0.05 and explored clusters of genes with similar expression patterns across sample groups using the 'degPatterns' function from the DEGreport R package. Gene lists associated with each identified cluster were used as input for functional enrichment analysis.

## Functional and pathway enrichment analysis

Genes with  $|LFC| > 1.0$  and FDR < 0.1 in the Wald test were explored using gene ontology (GO) functional enrichment analysis and KEGG (Kyoto Encyclopedia of Genes and Genomes) pathway enrichment analysis performed using the database for annotation, visualization and integrated discovery (DAVID) (<https://david.ncifcrf.gov/>).<sup>S12–S15</sup> Pathways or GO terms were considered significant at FDR-adjusted  $q$ -values < 0.05.

To investigate the biological relevance of clusters of DEGs associated with main expression patterns, we performed GO functional enrichment analysis using GOrilla, a publicly available GO enrichment tool (<http://cbl-gorilla.cs.technion.ac.il>).<sup>516</sup> GOrilla compares a target gene list (in this case, genes assigned to a given cluster) to a background set of genes ( $N = 2547$  genes significant in the LRT with  $FDR < 0.05$ ) and assesses the significance of enrichment for GO terms using the hypergeometric test.

## Results

### *Gastrocnemius and quadriceps muscle weights and morphology*

To assess potential sarcopenia onset in the C57BL/6JN mouse colony used for this study, we analysed the weights of two muscles: the gastrocnemius (innervated by the sciatic nerve) and the quadriceps (to evaluate a muscle innervated by another nerve, i.e., the femoral nerve). These were evaluated from a separate cohort of mice from the same NIA mouse colony (as these muscles were no longer available in the mice that had sciatic nerve RNA submitted for sequencing). Gastrocnemius weight (normalized to body weight) did not significantly differ across mice aged 5, 18, 21 and 24 months (global  $P = 0.062$ , one-way ANOVA) (Figure 1A), but there was a significant difference in the normalized weight of the quadriceps (global  $P = 0.0027$ , one-way ANOVA); Tukey's multiple comparisons test revealed a significant decrease in the normalized quadriceps weight of mice aged 21 months ( $P = 0.018$ ) and 24 months ( $P = 0.002$ ) compared with 5-month-old mice (Figure 1A). This suggests that with advancing age, the quadriceps was not fully capable of maintaining its mass in relation to increasing body weight (Figure S4).<sup>517</sup> However, we did not detect any significant age-related changes in the non-normalized weights of either the gastrocnemius (global  $P = 0.232$ , one-way ANOVA) or the quadriceps (global  $P = 0.197$ , one-way ANOVA), though we did observe a progressive, non-significant increase in the raw gastrocnemius weight with advancing age and a non-significant decrease in the raw quadriceps weight of mice aged 21 and 24 months compared with 5-month-old mice (Figure 1B). Collectively, these results demonstrate that although the quadriceps may have been less adapted to perform its weight-bearing task in heavier mice, overall, we did not observe overt decline in muscle mass in these mice. These results also support previous reports of only moderate or very small decreases in muscle mass in aging rat and mouse models compared with humans.<sup>518</sup>

We also analysed cross-sections of H&E-stained gastrocnemius and quadriceps muscles. Myofibers with centralized

myonuclei were counted as these may indicate continuous muscle degeneration and regeneration as observed in aging.<sup>519</sup> The number of centralized nuclei in gastrocnemius myofibers (expressed as a percentage of total myofiber number) was significantly higher in 24-month-old mice compared with 5-month-old mice (Figure 1C,  $P = 0.0076$ ). In the quadriceps, there was an increase in percentage of myofibers with centralized nuclei that did not reach statistical significance ( $P = 0.06$ ). However, as has been reported previously,<sup>5</sup> the number of myofibers with centralized nuclei was relatively low (<4% of the total myofiber number). The presence of centralized myonuclei beginning at 21 months can be seen in representative images of muscle cross-sections (Figure 1D, yellow arrowheads). We also qualitatively observed signs of low-grade inflammation, primarily in perivascular areas, in the cross-sections of mice aged 24 months, and to a lesser extent in mice aged 21 months, but not in younger mice (Figure 1D, blue arrowheads). This low-grade inflammation, which has been implicated in sarcopenia pathogenesis, was well illustrated by Sciorati and colleagues.<sup>520</sup>

Abnormal distribution of myofiber size is indicative of pathological changes in muscles.<sup>55</sup> Therefore, we expected muscles to show an abnormal proportion of small and large muscle fibres in the size-distribution histograms of older mice. To assess this, we sampled 300–600 muscle fibres per animal ( $n = 4$  per mice age group;  $\geq 1200$  myofibers assessed per group). For each myofiber present in a cross-sectional image, we calculated the minimal 'Feret's diameter' (i.e., the minimum distance of parallel tangents at opposing borders of the muscle fibre, measured in microns). The minimal 'Feret's diameter' distributions for 5-month-old and 24-month-old mice were significantly different for both gastrocnemius and quadriceps ( $P = 0.047$  and  $0.011$ , respectively; Figure S5). In gastrocnemius, the 24-month-old age group showed the largest coefficient of variation (CV) in minimal 'Feret's diameter' (CV = 0.26 at 24 months; 0.24 at 5 months). Taken together, the increase in centralized myonuclei, skewed distribution in myofiber size assessed by minimal 'Feret's diameter', and the observation of mis-shaped myofibers and inflammation in gastrocnemius and quadriceps cross-sections suggest pathological muscle aging starting at 21 months and progressing towards sarcopenia onset at 24 months in the C57BL/6JN mice used for this study. This pathological muscle aging was more advanced in the quadriceps muscle where a significant loss of muscle mass normalized to total body weight was measured. This confirms that our study of the sciatic nerve and corresponding gastrocnemius muscle between 18 and 24 months in C57BL/6JN females positions us ideally to investigate early molecular pathways occurring in peripheral nerves before overt sarcopenia and loss of mass in muscles innervated by this specific nerve.

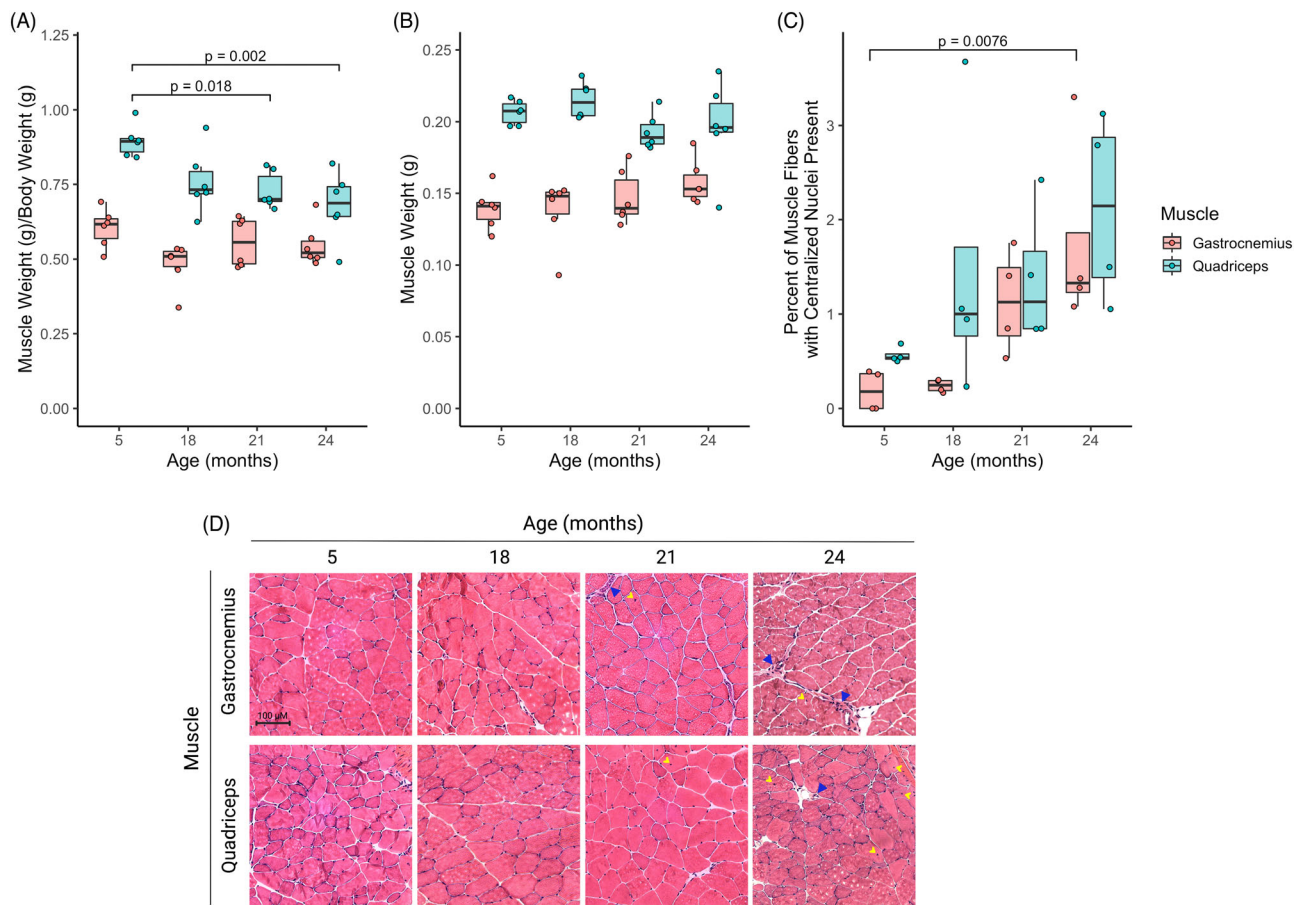


**Figure 1** Analysis of gastrocnemius and quadriceps muscle weights and morphology in a separate cohort of female C57BL/6JN mice aged 5–24 months. (A, B) Boxplots of muscle weight data in grams for  $n = 6$  mice per age group, shown normalized to total body weight in grams (A) or without normalization to total body weight (B).  $P$ -values indicate significantly different mean muscle weights ( $P < 0.05$ , analysis of variance with Tukey's test). (C) The proportion (%) of myofibers with non-peripheral myonuclei/total number of myofibers was quantified in haematoxylin and eosin (H&E)-stained cross-sections of gastrocnemius and quadriceps.  $P$ -values indicate significant differences ( $P < 0.05$ , Kruskal–Wallis with Dunnett's post hoc test) in the number of centralized myonuclei (expressed as a percentage of the total myofiber number) comparing each age with the reference group (5 months). (D) Images of H&E-stained myofiber cross-sections depict myofibers with uniform appearance at ages 5 and 18 months, and centralized myonuclei (yellow arrowheads) and low-grade inflammation in perivascular areas (blue arrowheads) at 24 months that is less pronounced at 21 months. Scale bar is 100  $\mu\text{M}$ . For (C) and (D),  $n = 4$  animals per group, with 300–600 myofibers assessed per animal across 7 images.

### Quantitative reverse transcription PCR of genes associated with neuromuscular junction denervation in gastrocnemius muscle

To validate myofiber denervation, which was previously demonstrated to correlate with the onset of sarcopenia in a C57BL/6J mouse strain, we performed qRT-PCR quantification of nicotinic acetylcholine receptor gamma and delta subunits (*Chrn $\gamma$*  and *Chrn $\delta$* ), runt-related transcription factor-1 (*Runx1*), growth arrest and DNA damage-inducible 45a (*Gadd45a*) and Myogenin (*Myog*) in gastrocnemius muscle. It has been previously established that increased expression of these genes in aging muscle is concomitant with the transition to sarcopenia in 24-month-old female C57BL/6J mice.<sup>5</sup> We observed significantly increased ex-

pression in *Chrn $\delta$*  and *Runx1* at 24 months compared with 5-month-old mice ( $P = 0.013$  and  $0.045$ , respectively) and a marginally significant increase ( $P < 0.1$ ) in expression of *Gadd45a* comparing 24-month-old mice with 5-month-old mice ( $P = 0.088$ ) (Figure S6). There was an increase in *Chrn $\gamma$*  and *Myog* expression at 24 months that was not statistically significant.

### Identification of differentially expressed genes in sciatic nerve by RNA sequencing

The number of DEGs ( $|\text{LFC}| > 1.0$ ,  $\text{FDR} < 0.05$ ) identified using DESeq2 is shown in Table 1. The full DESeq2 results, including the list of all genes and their associated LFC and

*P*-values, are shown in *Data S2*. Because we were interested in the earliest transcriptional changes that may precede initiation of myofiber pathology, we focused on the contrast between 18-month-old and 5-month-old mice. Comparing these two groups, a total of 51 DEGs were identified, including 28 up-regulated and 23 down-regulated DEGs (*Figure 2* and *Table 2*, listed in order of ascending *P*-value). The most up-regulated genes (according to LFC) were leiomodlin-2 (*Lmod2*, LFC = 7.52; FDR *q*-value = 0.001) and titin (*Ttn*, LFC = 6.80; FDR *q*-value = 0.014). The most down-regulated genes (according to LFC) were guanylate-binding protein 1 (*Gbp1*, LFC = -21.78; FDR *q*-value = 1.33E-24) and cadherin-6 (*Cdh6*; LFC = -21.38; FDR *q*-value = 1.33E-24). Volcano plots showing results of the other pairwise comparisons are shown in *Figure S7*.

To explore the biological roles of up- and down-regulated DEGs, we performed functional and pathway enrichment

**Table 1** Number (%) of differentially expressed genes (DEGs) out of 15 930 genes analysed

# DEGs FDR < 0.05		
Contrast	LFC > 1.0	LFC < -1.0
18 vs. 5 months	28 (0.176%)	23 (0.144%)
21 vs. 5 months	20 (0.126%)	6 (0.038%)
24 vs. 5 months	46 (0.289%)	16 (0.1%)
21 vs. 18 months	18 (0.113%)	7 (0.044%)
24 vs. 18 months	16 (0.1%)	6 (0.038%)
24 vs. 21 months	0 (0.0%)	1 (0.006%)

Abbreviations: FDR, false discovery rate; LFC, log<sub>2</sub> fold change.

analyses on the DEGs comparing 18-month-old (*n* = 5) and 5-month-old (*n* = 6) mice using DAVID. To expand the list of genes analysed to uncover potential pathways and hypotheses for future validation, we input into the analysis genes with |LFC| > 1.0 and FDR < 0.1. Up-regulated DEGs (54) were associated with KEGG pathways related to the AMP-activated protein kinase (AMPK) signalling pathway (FDR *q*-value = 0.02) and circadian rhythm (FDR *q*-value = 0.02) (*Table 3*). When restricting the analysis to only the 28 up-regulated DEGs (FDR < 0.05) listed in *Table 2*, only the AMPK signalling pathway remained statistically significant (FDR *q*-value = 0.0037; *Data S3*). ‘Circadian rhythm’ was also a significant GO Biological Process (BP) term (FDR *q*-value = 7.8E-4) of the 54 up-regulated genes with FDR < 0.1 and was borderline significant (FDR *q*-value = 0.055) for the 28 DEGs with FDR < 0.05. Other significant GO BP terms included ‘sarcomere organization’ (FDR *q*-value = 1.0E-6) and ‘muscle contraction’ (FDR *q*-value = 1.8E-6), among others (*Data S3*).

The 28 down-regulated DEGs (FDR < 0.1) comparing mice aged 18 months (*n* = 5) with mice aged 5 months (*n* = 6) were associated with various pathways related to biosynthetic processes, including terpenoid backbone biosynthesis (FDR *q*-value = 4.8E-5) and steroid biosynthesis (FDR *q*-value = 0.0034) as well as metabolic pathways (FDR *q*-value = 0.0055; *Table 3* and *Data S3*). Circadian rhythm was also enriched (*P* = 0.03, though it did not reach statistical significance after adjustment, FDR *q*-value = 0.29) among down-regulated genes including neuronal PAS domain protein 2 (*Npas2*) and the principal circadian clock gene encoding Aryl hydrocarbon re-

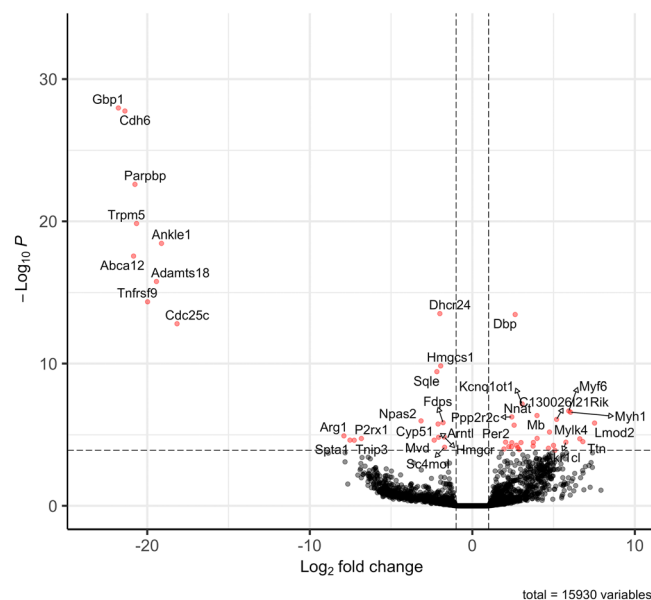


**Figure 2** Volcano plot of differentially expressed genes (of 15 930 genes analysed) in sciatic nerve comparing 18-month-old mice (*n* = 5) with 5-month-old mice (*n* = 6). The dashed line is the false discovery rate (FDR) *q*-value = 0.05. The 51 genes significant at |log<sub>2</sub> fold change| > 1.0 and FDR *q*-value < 0.05 (Wald test) are plotted in red.

**Table 2** The 51 differentially expressed genes identified in sciatic nerve comparing 18-month-old mice ( $n = 5$ ) with 5-month-old healthy, mature adult control mice ( $n = 6$ ), including 28 up-regulated genes and 23 down-regulated genes

	Gene	Log <sub>2</sub> fold change	FDR $q$ -value
Up-regulated	<i>Dbp</i>	2.63	5.55E-11
	<i>Kcnq1ot1</i>	3.06	7.56E-05
	<i>Myf6</i>	5.93	2.20E-04
	<i>Myh1</i>	6.04	2.52E-04
	<i>Nnat</i>	3.98	4.06E-04
	<i>Ppp2r2c</i>	2.43	4.83E-04
	<i>C130026I21Rik</i>	5.18	6.81E-04
	<i>Lmod2</i>	7.52	1.07E-03
	<i>Per2</i>	2.57	1.38E-03
	<i>Mb</i>	4.75	4.03E-03
	<i>Lars2</i>	3.98	9.59E-03
	<i>Mylk4</i>	6.61	9.76E-03
	<i>Ttn</i>	6.80	1.36E-02
	<i>Akr1cl</i>	5.76	1.41E-02
	<i>Tmem45b</i>	2.05	1.41E-02
	<i>Slc2a4</i>	2.99	1.41E-02
	<i>Fabp3</i>	3.75	1.41E-02
	<i>Zbtb16</i>	2.43	1.41E-02
	<i>Mybpc1</i>	4.99	2.09E-02
	<i>Pfkfb1</i>	2.71	2.09E-02
	<i>Rn45s</i>	3.74	2.29E-02
	<i>Plin4</i>	2.24	2.45E-02
	<i>Malat1</i>	2.41	2.49E-02
	<i>Till7</i>	2.80	2.71E-02
	<i>Tmem52</i>	4.68	2.90E-02
	<i>Col24a1</i>	1.95	3.21E-02
	<i>Lep</i>	2.88	3.47E-02
	<i>Tcap</i>	5.08	3.84E-02
Down-regulated	<i>Cdh6</i>	-21.38	1.33E-24
	<i>Gbp1</i>	-21.78	1.33E-24
	<i>Parpbp</i>	-20.76	1.31E-19
	<i>Trpm5</i>	-20.66	5.62E-17
	<i>Ankl1</i>	-19.13	1.08E-15
	<i>Abca12</i>	-20.84	7.05E-15
	<i>Adamts18</i>	-19.44	3.73E-13
	<i>Tnfrsf9</i>	-19.98	8.83E-12
	<i>Dhcr24</i>	-2.00	5.32E-11
	<i>Cdc25c</i>	-18.17	2.25E-10
	<i>Hmgcs1</i>	-1.95	1.92E-07
	<i>Sqle</i>	-2.18	4.56E-07
	<i>Npas2</i>	-3.16	8.23E-04
	<i>Fdps</i>	-1.80	1.05E-03
	<i>Cyp51</i>	-2.11	1.19E-03
	<i>Arg1</i>	-7.90	7.22E-03
	<i>Hmgcr</i>	-1.73	8.39E-03
	<i>Arntl</i>	-2.08	8.41E-03
	<i>P2rx1</i>	-6.83	9.59E-03
	<i>Spta1</i>	-7.53	1.12E-02
	<i>Tnip3</i>	-7.27	1.12E-02
	<i>Mvd</i>	-2.35	1.12E-02
	<i>Sc4mol</i>	-1.71	2.61E-02

Note: Differentially expressed genes in this table are sorted by ascending false discovery rate (FDR)  $q$ -value.

ceptor nuclear translocator-like protein 1 (*Arntl*). These two genes displayed similar gene expression patterns across age groups (Figure 3). There was no difference in KEGG pathway analysis results of down-regulated genes when restricting the analysis to the 23 down-regulated DEGs with FDR < 0.05. Significant GO BP terms of down-regulated genes

included 'sterol biosynthetic process' (FDR  $q$ -value = 3.5E-12), 'cholesterol biosynthetic process' (FDR  $q$ -value = 4.4E-9), 'cholesterol metabolic process' (FDR  $q$ -value = 5.3E-9), 'steroid biosynthetic process' (FDR  $q$ -value = 2.9E-8), 'steroid metabolic process' (FDR  $q$ -value = 6.2E-7), 'isoprenoid biosynthetic process' (FDR  $q$ -value = 4.8E-6) and 'lipid metabolic process' (FDR  $q$ -value = 5.5E-4). Again, these same GO BP terms remained significant when limiting to the 23 DEGs with FDR < 0.05 (Data S3).

### Validation of differentially expressed genes in sciatic nerve via quantitative reverse transcription PCR

We performed qRT-PCR on a set of DEGs to validate the RNA-seq results. As shown in Figure 4, gene expression in the sciatic nerve measured by qRT-PCR agreed with our RNA-seq findings. Compared with 5-month-old mice, there was an increase in expression of D site albumin promoter binding protein (*Dbp*,  $P = 0.022$ ) and the principal clock gene period circadian regulator 2 (*Per2*,  $P = 0.013$ ) in 18-month-old mice (Figure 4A,B). We also confirmed that the genes guanylate-binding protein 1 (*Gbp1*) and 24-dehydrocholesterol reductase (*Dhcr24*) were down-regulated in 18-month-old mice compared with 5-month-old mice ( $P = 0.043$  and  $P < 0.0001$ , respectively) (Figure 4C,D). qRT-PCR results for 13 additional genes we validated are shown in Figure S8.

### Pattern identification and functional enrichment analyses of clusters of differentially expressed genes

To investigate biologically relevant changes in gene expression across age groups, we analysed all pairwise comparisons of the normalized RNA-seq counts simultaneously using the LRT, which identified 2547 genes significant at FDR < 0.05. Using the 'degPatterns' function in R, we identified groups of genes within this list with similar expression patterns across age groups (henceforth referred to as 'clusters'). We identified seven clusters of genes containing 119–674 genes per cluster (Figure S9) and explored the biological relevance of these clusters using functional enrichment analysis assessing enrichment of clusters for GO BP terms (Figure 5).

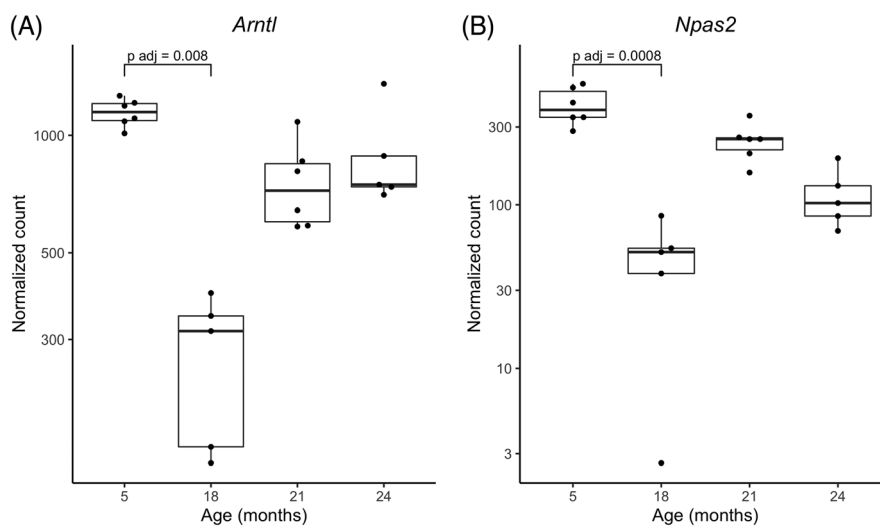
Cluster 1, containing 341 genes, was significantly enriched with genes associated with various biosynthetic and metabolic processes as well as 'extracellular matrix organization' (FDR  $q$ -value = 1.13E-03) and 'extracellular structure organization' (FDR  $q$ -value = 6.67E-04). Cluster 2 contained 536 genes associated with 'anterograde axonal transport' and 'organelle disassembly', but these did not reach statistical significance after adjustment for multiple comparisons. Cluster 3 (674 genes) was associated with 146 GO BP terms



**Table 3** Kyoto Encyclopedia of Genes and Genomes (KEGG) pathway analysis of 54 up- and 28 down-regulated differentially expressed genes with false discovery rate (FDR) < 0.1, comparing 18-month-old mice ( $n = 5$ ) with 5-month-old mice ( $n = 6$ )

KEGG pathway	Gene count	P-value	FDR $q$ -value	Genes	
Up-regulated	AMPK signalling pathway	4	5.50E-04	2.00E-02	<i>Pfkfb1, Lep, Ppp2r2c, Slc2a4</i>
	Circadian rhythm	3	7.00E-04	2.00E-02	<i>Bhlhe41, Per2, Per3</i>
	Fructose and mannose metabolism	2	4.50E-02	5.40E-01	<i>Pfkfb1, Aldob</i>
Down-regulated	Terpenoid backbone biosynthesis	4	1.30E-06	4.80E-05	<i>Hmgcr, Hmgcs1, Fdps, Mvd</i>
	Steroid biosynthesis	3	1.80E-04	3.40E-03	<i>Dhcr24, Cyp51, Sqle</i>
	Metabolic pathways	8	4.30E-04	5.50E-03	<i>Dhcr24, Hmgcr, Hmgcs1, Arg1, Cyp51, Fdps, Mvd, Sqle</i>
	Circadian rhythm	2	3.00E-02	2.90E-01	<i>Arntl, Npas2</i>

Note: For up-regulated genes, only shown are pathways significant at  $P$ -value < 0.05. Abbreviation: AMPK, AMP-activated protein kinase.

**Figure 3** Expression of *Arntl* (A) and *Npas2* (B) in sciatic nerve of mice aged 5, 18, 21 and 24 months. Plot of normalized DESeq2 counts of *Arntl* and *Npas2* in sciatic nerve of mice aged 5 ( $n = 6$ ), 18 ( $n = 5$ ), 21 ( $n = 6$ ) and 24 ( $n = 5$ ) months. False discovery rate (FDR)  $q$ -values denoted on the graph are for comparisons significant (FDR < 0.05) in the Wald test.

(FDR < 0.05). Genes in Cluster 3 were associated with GO BP terms such as 'immune system process' (FDR  $q$ -value = 6.9E-10), 'immune response' (FDR  $q$ -value = 1.73E-07) and 'regulation of immune system process' (FDR  $q$ -value = 2.93E-07). Cluster 4 (529 genes) was associated with 80 GO BP terms (FDR < 0.05). Significantly enriched GO BP terms included 'muscle system process' (FDR  $q$ -value = 2.05E-04), 'striated muscle contraction' (FDR  $q$ -value = 1.73E-04), 'muscle contraction' (FDR  $q$ -value = 1.26E-04) and various metabolic processes. None of the GO terms in Cluster 5 (165 genes) reached statistical significance after adjustment for multiple comparisons. The 119 genes in Cluster 6 were associated with 62 GO BP terms mainly related to immune system processes and the defence response (e.g., 'response to external biotic stimulus', 'response to bacterium', 'response to stress' and 'response to chemical'). Lastly, the 183 genes in Cluster 7 were involved in 'translation' (FDR  $q$ -value = 5.47E-15) and

related processes as well as cell cycle processes. The full results of this analysis are available in *Data S4*.

## Discussion

Sarcopenia is the pathological age-associated progressive decline in skeletal muscle mass and strength.<sup>7</sup> Although sarcopenia has long been considered a disease of skeletal muscle fibres only, accumulating evidence suggests that sarcopenia may originate in the nervous system through a loss of alpha motor neuron axons and the fibre type grouping that results from the concomitant remodelling of motor units, as reviewed by Gustafsson and Ulfhake.<sup>8</sup> Molecular and structural alterations at the NMJ have also been observed,<sup>8,9</sup> but it is unclear whether alteration of motor units or NMJs is one of the first stages leading to sarcopenia.

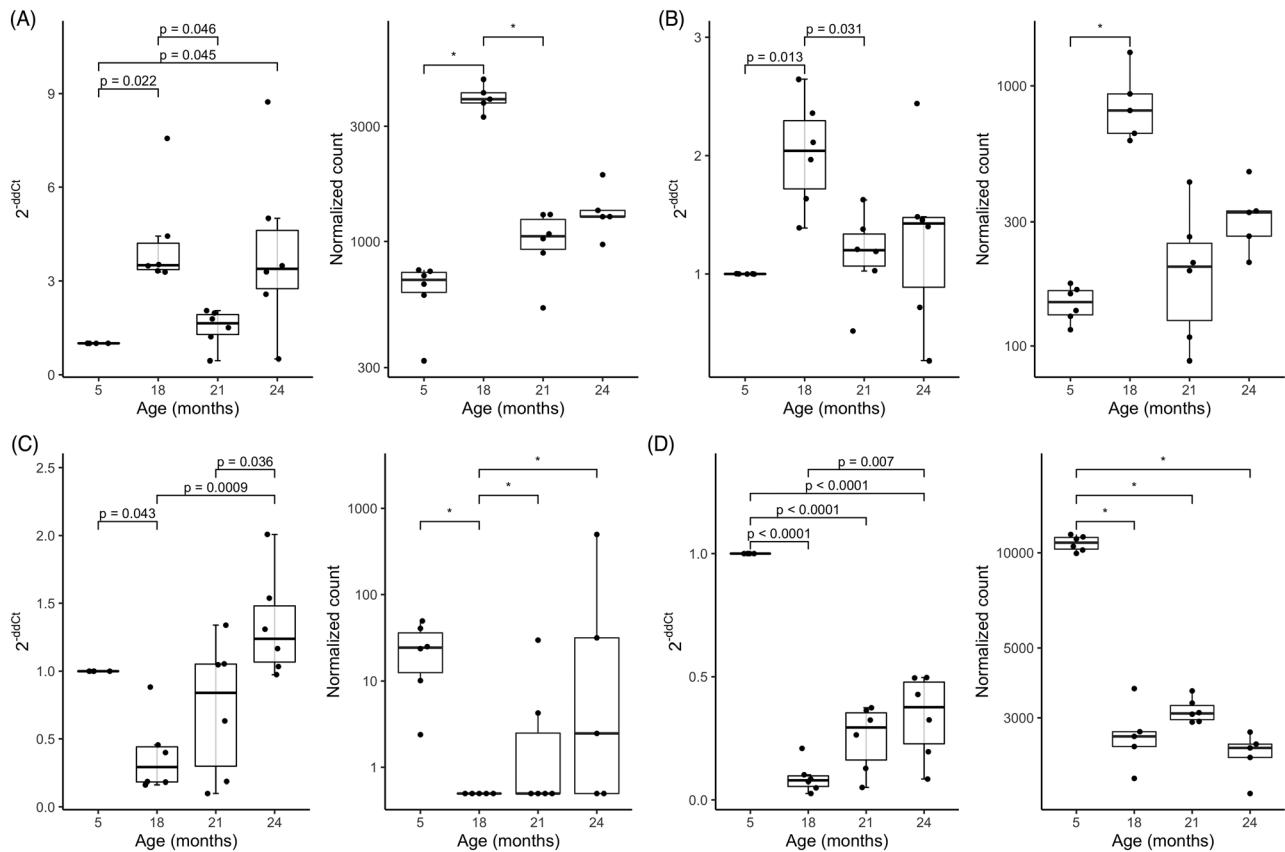


**Figure 4** Expression of *Dbp* (A), *Per2* (B), *Gbp1* (C) and *Dhcr24* (D) in sciatic nerve of mice aged 5, 18, 21 and 24 months ( $n = 5-6$  per age group) assessed by quantitative real-time PCR (qRT-PCR, left) and RNA sequencing (RNA-seq, right). Left: Relative gene expression assessed by qRT-PCR. The delta-delta cycle threshold (ddCt) was calculated using *Ppia* and *Hprt* housekeeping genes with 5-month-old mice used as the reference.  $P$ -values were calculated from one-way analysis of variance followed by Tukey's test. Right: Corresponding plot of normalized counts from RNA-seq analysis. Asterisk denotes statistical significance (false discovery rate  $q$ -value < 0.05) in the Wald test.

This study demonstrates that gene expression changes in the sciatic nerve relevant to sarcopenia can be detected prior to clinical onset of myofiber denervation and sarcopenia in muscle. We showed that expression of genes previously implicated in sarcopenia, such as the principal clock gene *Arntl* (also known as *Bmal1*),<sup>10</sup> is differentially expressed ( $|LFC| > 1.0$ ,  $FDR < 0.05$ ) in nerve as early as 18 months of age compared with healthy, mature adult controls. Pathway enrichment analysis revealed that up-regulated DEGs at 18 months were associated with the AMPK signalling pathway whereas down-regulated DEGs were associated with biosynthesis and metabolic pathways. Both up- and down-regulated DEGs were associated with circadian rhythm genes, suggesting that this is a particularly important pathway in aging sciatic nerve.

Our hypothesis that alterations in peripheral nerves occur prior to the clinical expression of sarcopenia is supported by a previous longitudinal study in C57BL/6J mice (aged between 4 and 24 months) that measured significant accumulation of a series of proteins implicated in cytoskeleton dynamics/axonal transport and autophagic protein degradation

pathways in the sciatic nerve starting at 18 months,<sup>1</sup> whereas in the same mice, loss of muscle mass and denervation at the NMJ was only clearly substantiated by 24 months of age.<sup>5,11</sup> Furthermore, prior work has reported signs of sarcopenia in C57BL/6J mice (such as changes in muscle volume, weights, cross-sectional area and measures of muscle function) as early as ~20 months of age,<sup>12</sup> yet most studies utilizing the naturally aging C57BL/6J mouse model of sarcopenia study mice older than 24 months of age,<sup>13</sup> obscuring the study of molecular mechanisms early in the disease course. Here, we report altered expression of several key genes in the nerve as early as 18 months.

The top up-regulated DEGs (by LFC) are *Lmod2* and *Ttn*, genes that play roles in sarcomere organization and maintaining sarcomere integrity. Increased expression of genes such as *Myf6*, *Myh1*, *Mb*, *Mylk4*, *Mybpc1* and *Tcap* (Table 2) further suggests that the expression changes detected are relevant to muscle function. Differential expression of cell-cell adhesion and junction assembly/organization gene *Cdh6* and cytoskeleton and extracellular matrix genes *Fabp3*, *Ttll7*, *Col24a1*, *Adamts18* and *Spta1* suggests dynamic changes at

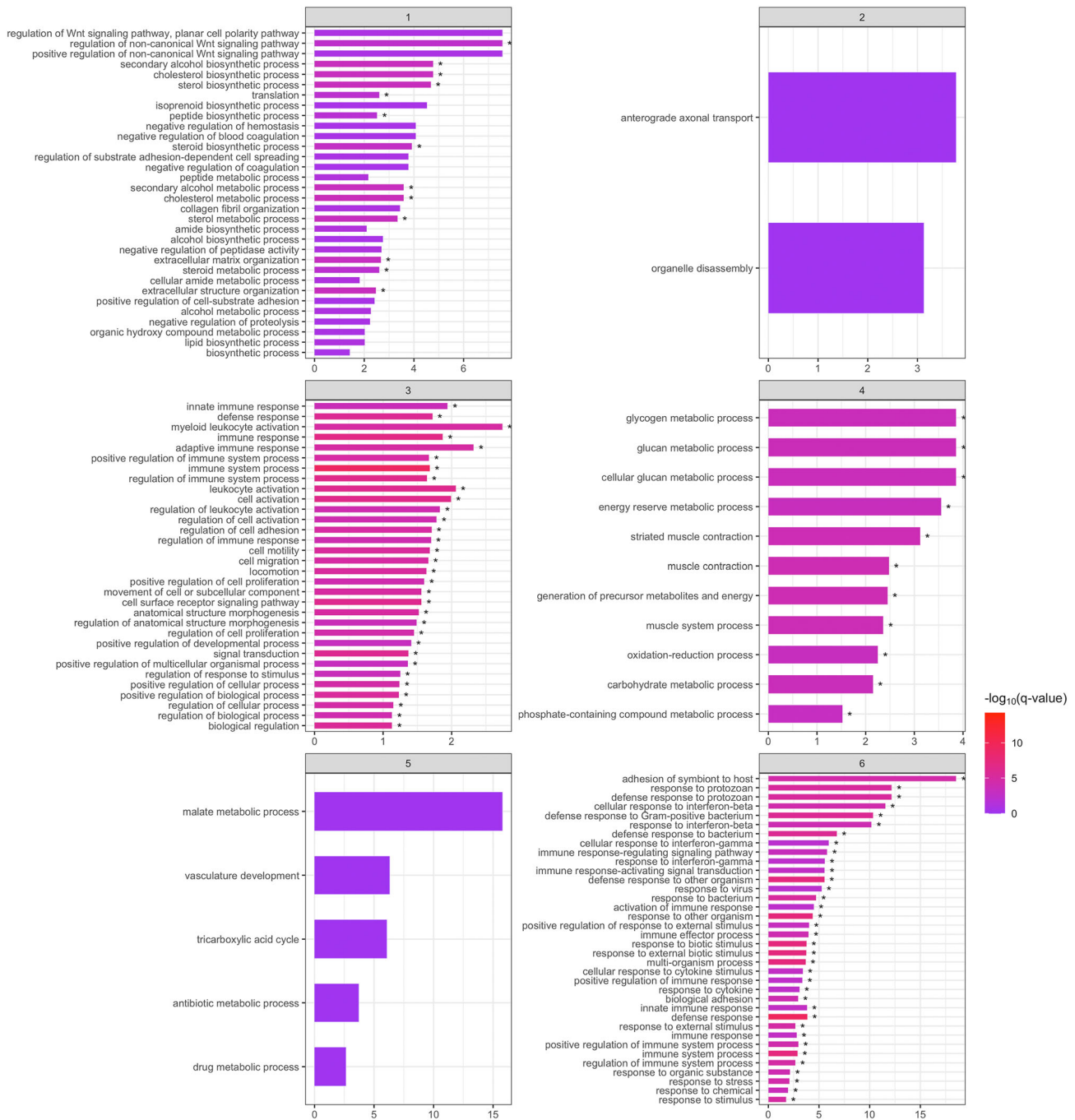


**Figure 5** Gene Ontology Biological Process (GO BP) functional enrichment analysis of the seven clusters of gene expression, denoted in grey, identified by the 'degPatterns' R package. The enrichment score is shown on the y axis, with bars coloured according to  $-\log_{10}(q\text{-value})$ . \*GO BP terms significantly enriched with target genes, false discovery rate (FDR)  $q\text{-value} < 0.05$ . For Clusters 3 and 4, only GO BP terms significant at FDR < 0.001 are shown. For Cluster 6, only GO BP terms significant at FDR < 0.01 are shown.

the NMJ. *Trpm5* was among the top down-regulated DEGs. TRPM5, an integral component of the plasma membrane, contributes to postural tone in hindlimbs of mice and motor output during locomotion.<sup>14</sup> The involvement of these DEGs in sarcopenia development deserves further investigation as

the study of these genes may increase our understanding of the disease aetiology and identify potential therapeutic targets.

Functional and pathway enrichment analysis identified circadian rhythm as a key pathway targeted by the DEGs. We

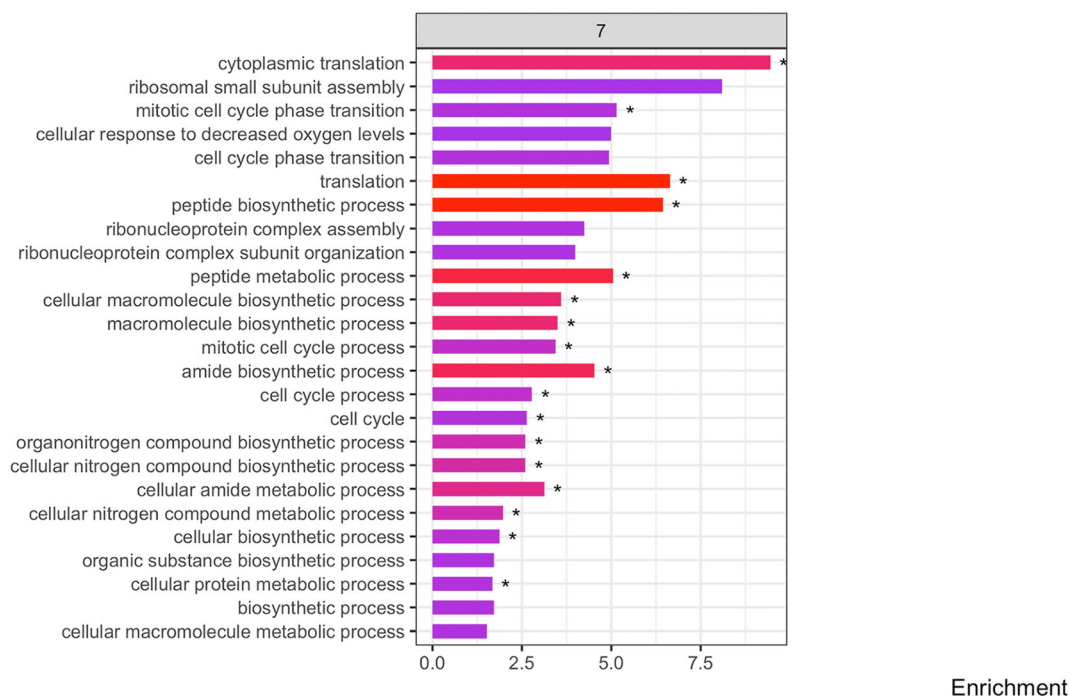


Figure 5 Continued

detected significant down-regulation of *Arntl*, a core component of the principal clock, in sciatic nerve at 18 months of age. Mice deficient in brain and muscle *Arntl* have reduced lifespans and show symptoms of premature aging including sarcopenia.<sup>10</sup> We found dysregulation in other circadian clock genes, including period circadian regulator 2 and 3 (*Per2* and *Per3*) and *Npas2*. Molecular clock disruptions are linked to aging and the development of many chronic diseases including sarcopenia.<sup>15</sup> For example, circadian rhythm disruption was associated with an increased risk of sarcopenia in a study comparing the risk of sarcopenia between night-shift workers and those who never worked night shifts.<sup>16</sup> Our results suggest that impaired circadian rhythm maintenance may be important in sarcopenia development.

The AMPK signalling pathway was identified as an important pathway among up-regulated DEGs. AMPK activation positively regulates signalling pathways that replenish cellular ATP supplies, including autophagy. Indeed, one gene that we identified through functional pattern analysis was the mitophagy protein BCL2 Interacting Protein 3 (*Bnip3*). *Bnip3* inhibition protects against muscle wasting,<sup>17</sup> yet we detected an increase in *Bnip3* expression in sciatic nerve at 18 months, which we confirmed with qRT-PCR (Figure S8). We also detected increased expression of PTEN-induced kinase 1 (*Pink1*), which encodes an essential pro-survival factor of mitochondria in the face of pathologic oxidative stress.<sup>18</sup> Thus, the up-regulation at 18 months (confirmed with qRT-PCR) could reflect a compensatory mechanism of damaged mito-

chondria or mitochondria being targeted for degradation due to aberrant AMPK signalling. Small molecule activators of PINK1 are in development<sup>19</sup> and perhaps could represent a future therapeutic strategy for sarcopenia. Aging-related mitochondria dysfunction (e.g., due to the build-up of reactive oxidative stress) may contribute to sarcopenia through increased apoptosis, reduced capacities for muscle regeneration or motor neuron cell death, as reviewed by Lo and colleagues<sup>20</sup> and Wiedmer and colleagues.<sup>21</sup> Furthermore, it has been shown that mitophagy and cell survival are regulated by the circadian *Clock* gene in cardiac myocytes,<sup>22</sup> suggesting that regulation of mitophagy in the context of sarcopenia may possibly be accomplished by the differentially expressed circadian genes we identified. The up-regulation of mitochondrial genes including *Bnip3* and *Pink1* suggests an important role of the mitochondria in sarcopenia onset in peripheral nerves that deserves further exploration, as well as the regulation of mitophagy by circadian clock genes.

AMPK activation also negatively regulates ATP-consuming biosynthetic processes such as protein synthesis. This agrees with our finding of down-regulation of biosynthetic and metabolic pathways and a previous study<sup>1</sup> that observed an accumulation of proteins in sciatic nerve (with age, comparing 26- with 3-month-old female C57BL/6J mice) suggesting age-related dysfunction of degradation mechanisms, which may possibly reduce synaptic efficacy and muscle contractability through impaired axonal transport, excitability and neurotransmitter supply to NMJs. AMPK signalling has

also been implicated in several species as a critical modulator of aging<sup>23</sup> and is a candidate for the treatment of sarcopenia.<sup>20,24</sup>

Lastly, we performed functional enrichment analysis on clusters of genes with similar patterns of expression across age groups. Clusters 1 and 6 as well as 4 and 5 were of particular interest given their decrease and increase in expression at 18 months, respectively, which corresponds to the pre-onset of myofiber denervation in our C57BL/6JN mice. Cluster 1 genes were associated with biosynthetic and metabolic processes as well as with extracellular matrix organization and extracellular structure organization, suggestive of tissue remodelling with age and/or diminished remodelling capacity with aging.<sup>8</sup> The genes in Cluster 6 were associated with the immune system and defence response. Interestingly, Cluster 6 genes showed a large decrease in expression at 18 months that could indicate a window of immune vulnerability of the peripheral nervous system to external stimuli followed by a steady increase thereafter that could reflect immune system senescence associated with excessive proinflammatory cytokine production that some have referred to as 'inflammaging'.<sup>25</sup> Whether the drop in immune defences observed at 18 months is implicated in sarcopenia onset remains to be determined. Cluster 4 genes were associated with metabolic processes such as glycogen metabolism, glucan metabolism and energy reserve metabolic processes (among others), again suggesting dysfunctional AMPK signalling.

To our knowledge, this is the first report assessing the transcriptome of sciatic nerves in the context of sarcopenia using untargeted RNA-seq. The main strengths of this study include the use of an unbiased bioinformatics analysis, validation of RNA-seq findings using qRT-PCR and the use of multiple time points during the mouse lifespan preceding disturbances in myofiber innervation and overt sarcopenia with multiple ( $n = 5-6$ ) biological replicates. In our morphological assessment of myofiber cross-sections, we measured the minimal 'Feret's diameter' as this was previously shown to be the most robust geometrical parameter for cross-sectional muscle fibre size measurement that is the least influenced by experimental errors.<sup>55</sup> However, this study has several limitations. The main limitation of this study is that although we validated the onset of pathological skeletal muscle aging (occurring at 21 months, via analysis of gastrocnemius and quadriceps muscle weights and morphology) in a cohort of female C57BL/6JN mice from the NIA mouse colony, we did not validate the functional onset of sarcopenia (i.e., we did not assess muscle mass, strength, function, contractility etc.) in the cohort of mice utilized for the RNA-seq analyses. In these mice, we validated myofiber denervation at 24 months by replicating previous findings by Barns and colleagues.<sup>5</sup> Specifically, we found that expression of genes associated with NMJ denervation including *Chrnd*, *Runx1* and *Gadd45a* is up-regulated in the muscle of our female

C57BL/6JN mice aged 24 months ( $P < 0.1$ ). We did not detect significant up-regulation of *Chrng* or *Myog*, although there was a non-significant increase in expression compared with expression in 5-month-old mice. However, it is not clearly established that these markers can validate sarcopenia without other measures of sarcopenia such as changes in muscle mass, motor unit losses and muscle contractility changes. Although it has been previously established that increased expression of these molecular markers of myofiber denervation in aging muscle is concomitant with the transition to sarcopenia in 24-month-old female C57BL/6J mice,<sup>5</sup> we note that the mice used in the study by Barns and colleagues were not from the NIA colony but from an aging colony from Royal Brisbane Hospital in Queensland, Australia. The lifespan and healthspan (including sarcopenia onset) of mouse models of aging may differ from cohort to cohort due to spontaneous mutations as well as differences in technical factors such as differing housing and environmental conditions. Therefore, future studies should re-assess these markers alongside validated measures of sarcopenia such as muscle weight, function, contractile velocity and cross-sectional myofiber size.<sup>1,2,5,26</sup>

Given that previous studies have characterized female C57BL/6J mice, our study was also limited to females to facilitate comparison of the results, but future studies should be performed to thoroughly characterize sarcopenia development in male C57BL/6J mice. Thus, the generalizability of these results is limited to female mice from the NIA C57BL/6JN mouse colony. Also, the gastrocnemius muscles used for qRT-PCR to confirm myofiber denervation were dissected from snap-frozen legs. Although great measures were taken to ensure there was no contamination from other muscles (which may show variable susceptibility to aging), it is still possible that there may be minimal contamination from nearby muscles such as the plantaris and soleus muscles. However, we find it reassuring that our qRT-PCR results in gastrocnemius muscle not only are in alignment with data reported by Barns and colleagues in quadriceps (with up-regulation of genes associated with NMJ denervation) but also are supported by our findings of muscle weights in mice from the same NIA colony; in mice from the NIA colony used for our study, we observed less striking increases in gene expression in markers of myofiber denervation in gastrocnemius compared with what was previously reported in quadriceps (in mice from the Royal Brisbane Hospital). In agreement, in our mice, the gastrocnemius did not show statistically significant declines in normalized weight with aging whereas in quadriceps we observed a significant decrease in muscle mass normalized to total body weight. Muscle weight normalized to total body weight reflects the ability of a muscle to maintain muscle mass in relation to body weight and thus is a measure of how well adapted a muscle is in performing its weight-bearing task.<sup>517</sup> This further demonstrates that different muscles are impacted by the aging process to vary-

ing degrees (which could be impacted by factors such as muscle location, specific function or fibre type composition) and suggests that the quadriceps may be more susceptible to age-related muscle pathology in these mice.

Lastly, another limitation is that we performed RNA-seq on total RNA isolated from the entire sciatic nerve as opposed to pure motor nerves. Because the sciatic nerve is a mixed-function nerve, we sequenced some sensory axons in addition to motor axons. Interestingly, the sympathetic nervous system has recently gained attention for its role in regulating skeletal muscle motor innervation and its potential implication in sarcopenia pathogenesis.<sup>27</sup> Glial cells, including Schwann cells that myelinate peripheral axons, are in close contact with neurons within the sciatic nerve and so we measured some changes relevant to glia. Glial cells have also been proposed to play a leading role in neuromuscular aging and sarcopenia.<sup>28</sup> Changes in Schwann cell phenotype and plasticity have been observed in aged sciatic nerve of C57BL/6J mice.<sup>1,29</sup> Thus, age-related alterations in glial cells including Schwann cells may affect axonal function and stability at the NMJ and contribute to sarcopenia initiation.<sup>8</sup> Future studies could use novel spatial imaging techniques such as the RNAScope™ to untangle the cellular origin of the key molecular changes we report here.

In conclusion, we detected gene expression changes in the nerve as early as 18 months of age, prior to the onset of myofiber denervation, which we confirmed at 24 months by up-regulation of *Chrnd*, *Chrng*, *Gadd45a*, *Myog* and *Runx1* in muscle by qRT-PCR, and prior to age-related muscle pathology, which we confirmed at 24 months of age in a separate mouse cohort by an increase in fibres with centralized myonuclei and altered myofiber size distribution. Our results suggest that pathophysiological processes contributing to sarcopenia may be unfolding early in the nerve. We identified several genes and pathways that may represent possible targets for the prevention and treatment of sarcopenia. Increased understanding of how these pathways contribute to the aging process in nerve and skeletal muscle, and the mechanisms regulating skeletal muscle denervation at the NMJ, could be critical in identifying novel treatments and biomarkers for sarcopenia. Future studies examining longitudi-

nal gene expression profiles in peripheral nerves and the muscles they innervate at adult, early-sarcopenic and confirmed sarcopenic stages will be highly valuable and confirm the role of nerves in sarcopenia pathogenesis.

## Acknowledgements

The authors of this manuscript certify that they comply with the ethical guidelines for authorship and publishing in the *Journal of Cachexia, Sarcopenia and Muscle*.<sup>30</sup> This work was supported by the National Institutes of Health (NIH) National Institute on Aging (NIA) Grant (R21AG052011) awarded to D.B.R. and S.K., the National Institute of Environmental Health Sciences (NIEHS) Grant (ES009089) and the Ruth L. Kirschstein National Research Service Award Individual Pre-doctoral Fellowship (F31ES030973, awarded to N.C.). S.C., H.J.R., D.A. and A.M. are supported by the European Union's Horizon 2020 Research and Innovation Programme under the Marie Skłodowska-Curie grant agreement (No. 778003, awarded to S.C.). This research was also funded in part through the National Cancer Institute (NCI) Cancer Center Support Grant (P30CA013696) and used the Genomics and High Throughput Screening Shared Resource. We thank Chaolin Zhang for his assistance in interpreting the RNA-seq data and the NIA Aged Rodent Colonies and Tissue Bank for providing the mice and tissues used for the study.

## Conflict of interest

The authors have declared that they have no competing interests.

## Online supplementary material

Additional supporting information may be found online in the Supporting Information section at the end of the article.

## References

1. Krishnan VS, White Z, McMahon CD, Hodgetts SI, Fitzgerald M, Shavlakadze T, et al. A neurogenic perspective of sarcopenia: time course study of sciatic nerves from aging mice. *J Neuropathol Exp Neurol* 2016;**75**:464–478.
2. Pannérec A, Springer M, Migliavacca E, Ireland A, Piasecki M, Karaz S, et al. A robust neuromuscular system protects rat and human skeletal muscle from sarcopenia. *Aging (Albany NY)* 2016;**8**:712–728.
3. Ryall JG, Schertzer JD, Lynch GS. Cellular and molecular mechanisms underlying age-related skeletal muscle wasting and weakness. *Biogerontology* 2008;**9**:213–228.
4. Zhou J, Liao Z, Chen J, Zhao K, Xiao Q. Integrated study on comparative transcriptome and skeletal muscle function in aged rats. *Mech Ageing Dev* 2018;**169**:32–39.
5. Barns M, Gondro C, Tellam RL, Radley-Crabb HG, Grounds MD, Shavlakadze T. Molecular analyses provide insight into mechanisms underlying sarcopenia and myofibre denervation in old skeletal muscles of mice. *Int J Biochem Cell Biol* 2014;**53**:174–185.
6. Shavlakadze T, McGeachie J, Grounds MD. Delayed but excellent myogenic stem cell response of regenerating geriatric skeletal muscles in mice. *Biogerontology* 2010;**11**:363–376.
7. Cruz-Jentoft AJ, Sayer AA. Sarcopenia. *Lancet* 2019;**393**:2636–2646.

8. Gustafsson T, Ulfhake B. Sarcopenia: what is the origin of this aging-induced disorder? *Front Genet* 2021;**12**:688526.
9. Bao Z, Cui C, Chow SK, Qin L, Wong RMY, Cheung W. AChRs degeneration at NMJ in aging-associated sarcopenia—a systematic review. *Front Aging Neurosci* 2020;**12**:597811.
10. Kondratov RV, Kondratova AA, Gorbacheva VY, Vykhovanets OV, Antoch MP. Early aging and age-related pathologies in mice deficient in BMAL1, the core component of the circadian clock. *Genes Dev* 2006;**20**:1868–1873.
11. Chai RJ, Vukovic J, Dunlop S, Grounds MD, Shavlakadze T. Striking denervation of neuromuscular junctions without lumbar motoneuron loss in geriatric mouse muscle. *PLoS ONE* 2011;**6**:e28090.
12. Kim C, Hwang J-K. The 5,7-dimethoxyflavone suppresses sarcopenia by regulating protein turnover and mitochondria biogenesis-related pathways. *Nutrients* 2020;**12**:E1079.
13. Xie W-Q, He M, Yu D-J, Wu Y-X, Wang X-H, Lv S, et al. Mouse models of sarcopenia: classification and evaluation. *J Cachexia Sarcopenia Muscle* 2021;**12**:538–554.
14. Bos R, Drouillas B, Bouhadfane M, Pecchi E, Trouplin V, Korogod SM, et al. Trpm5 channels encode bistability of spinal motoneurons and ensure motor control of hindlimbs in mice. *Nat Commun* 2021;**12**:6815.
15. Vitale J, Bonato M, La Torre A, Banfi G. The role of the molecular clock in promoting skeletal muscle growth and protecting against sarcopenia. *Int J Mol Sci* 2019;**20**:4318.
16. Choi YI, Park DK, Chung J-W, Kim KO, Kwon KA, Kim YJ. Circadian rhythm disruption is associated with an increased risk of sarcopenia: a nationwide population-based study in Korea. *Sci Rep* 2019;**9**:12015.
17. Oost LJ, Kustermann M, Armani A, Blaauw B, Romanello V. Fibroblast growth factor 21 controls mitophagy and muscle mass. *J Cachexia Sarcopenia Muscle* 2019;**10**:630–642.
18. Wang N, Zhu P, Huang R, Wang C, Sun L, Lan B, et al. PINK1: the guard of mitochondria. *Life Sci* 2020;**259**:118247.
19. Miller S, Muqit MMK. Therapeutic approaches to enhance PINK1/Parkin mediated mitophagy for the treatment of Parkinson's disease. *Neurosci Lett* 2019;**705**:7–13.
20. Lo JH, Kin Pong U, Yiu T, Ong MTY, Lee WYW. Sarcopenia: current treatments and new regenerative therapeutic approaches. *J Orthop Translat* 2020;**23**:38–52.
21. Wiedmer P, Jung T, Castro JP, Pomatto LCD, Sun PY, Davies KJA, et al. Sarcopenia—molecular mechanisms and open questions. *Ageing Res Rev* 2021;**65**:101200.
22. Rabinovich-Nikitin I, Rasouli M, Reitz CJ, Posen I, Margulets V, Dhingra R, et al. Mitochondrial autophagy and cell survival is regulated by the circadian Clock gene in cardiac myocytes during ischemic stress. *Autophagy* 2021;**17**:3794–3812.
23. Mallick A, Gupta BP. AXIN-AMPK signaling: implications for healthy aging. *F1000Res* 2021;**10**:101259.
24. Feike Y, Zhijie L, Wei C. Advances in research on pharmacotherapy of sarcopenia. *Ageing Med* 2021;**4**:221–233.
25. Deleidi M, Jäggle M, Rubino G. Immune aging, dysmetabolism, and inflammation in neurological diseases. *Front Neurosci* 2015;**9**:172.
26. Graber TG, Kim J-H, Grange RW, McLoon LK, Thompson LV. C57BL/6 life span study: age-related declines in muscle power production and contractile velocity. *Age (Dordr)* 2015;**37**:9773.
27. Delbono O, Rodrigues ACZ, Bonilla HJ, Messi ML. The emerging role of the sympathetic nervous system in skeletal muscle motor innervation and sarcopenia. *Ageing Res Rev* 2021;**67**:101305.
28. Kwan P. Sarcopenia: the gliogenic perspective. *Mech Ageing Dev* 2013;**134**:349–355.
29. Painter MW, Brosius Lutz A, Cheng Y-C, Latremoliere A, Duong K, Miller CM, et al. Diminished Schwann cell repair responses underlie age-associated impaired axonal regeneration. *Neuron* 2014;**83**:331–343.
30. von Haehling S, Morley JE, Coats AJS, Anker SD. Ethical guidelines for publishing in the Journal of Cachexia, Sarcopenia and Muscle: update 2021. *J Cachexia Sarcopenia Muscle* 2021;**12**:2259–2261.